

Strontium Nitrate Extraction to Ionic Liquids by a Crown Ether: A Molecular Dynamics Study of Aqueous Interfaces with C₄mim⁺- vs C₈mim⁺-Based Ionic Liquids

A. Chaumont and G. Wipff*

Laboratoire MSM, Institut de Chimie, UMR CNRS 7177, Université de Strasbourg, 4, rue B. Pascal, 67 000 Strasbourg, France

Received: July 12, 2010; Revised Manuscript Received: August 24, 2010

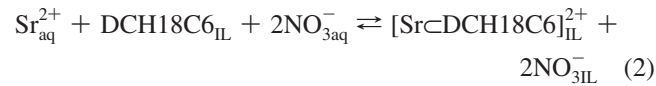
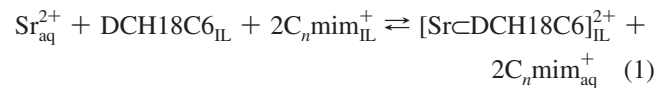
In order to gain microscopic insights into the extraction mechanism of strontium cations by 18-crown-6 (18C6) to room temperature ionic liquids (ILs), we simulated by molecular dynamics (MD) strontium complexes in neat ionic liquids and at their interfaces with water. We compared two ILs, based on the PF₆⁻ anion and either 1-butyl-3-methylimidazolium (C₄mim⁺) or 1-octyl-3-methylimidazolium (C₈mim⁺) cations. Regarding the complexes, two states were considered: charged [Sr \subset 18C6]²⁺ vs neutral [Sr \subset 18C6,(NO₃)₂], where the nitrates are either fully dissociated or coordinated to Sr. In “dry” or “humid” [C₄mim][PF₆] and in “dry” [C₈mim][PF₆] IL, the neutral complex is found to be the most stable one. In the binary IL/water solutions, the charged complexes mostly partition to the aqueous phase, whereas the neutral [Sr \subset 18C6,(NO₃)₂] complexes are more concentrated in the interfacial domain. The aqueous solutions in contact with the ionic liquids contain C₄mim⁺, but almost no C₈mim⁺ ions, supporting a classical extraction mechanism to [C₈mim][PF₆] and an ion exchange mechanism to [C₄mim][PF₆]. Furthermore, remarkable events occurred during the dynamics, where complexes were extracted to the IL phases. When compared to the interfacial landscapes obtained with the same solutes at a classical organic liquid (chloroform)/water interface, those with ILs allow us to better understand specific features of liquid–liquid extraction to ILs.

Introduction

The first synthesis of an air and water stable room temperature ionic liquid (IL) in 1992 by Wilkes et al.¹ opened the road for hydrophobic ILs to be used in biphasic systems.^{2,3} These ILs are typically based on organic cations (e.g., imidazolium, quaternary ammonium, and pyridinium derivatives) and X⁻ anions whose hydrophilic/hydrophobic balance mainly determines the IL miscibility with water. For instance, imidazolium-based ILs with hexafluorophosphate (PF₆⁻) or bis(trifluoromethylsulfonyl)imide (Tf₂N⁻) anions form biphasic systems with water and can be used for separation of metallic cations by liquid–liquid extraction (LLE), generally using “traditional” extractant molecules.^{4–6} Crown ethers^{7–9} and calix[4]arenes¹⁰ extract alkali cations, phosphoryl-containing CMPO and TBP ligands extract f-ions like Pu⁴⁺, Th⁴⁺, Am³⁺, and UO₂²⁺, dialkylphosphoric (HDEHP) or dialkylphosphonic acids extract UO₂²⁺ and trivalent lanthanide and actinide ions such as Am³⁺, Nd³⁺, and Eu³⁺.^{11,12} A remarkable result with ILs is the drastic increase of the extraction coefficients, when compared to “classical” organic solvents like kerosene, chloroform, or octanol. More recently, task-specific ionic liquids, where the extractant moiety is grafted on the IL cation, have been developed with success to extract metal ions.^{13–15}

One of the most extensively investigated LLE system deals with the Sr²⁺ cation extraction by crown ethers (CE). In 1999 Dai et al.¹⁶ reported that extraction by dicyclohexyl-18-crown-6 (DCH18C6) toward imidazolium based ILs leads to partition coefficient D_{Sr} 10–10 000 times higher than toward “classical” solvents (toluene or chloroform). Even without DCH18C6, D_{Sr} values are in the order of magnitude of those observed for classical solvents with DCH18C6. With the DCH18C6 extrac-

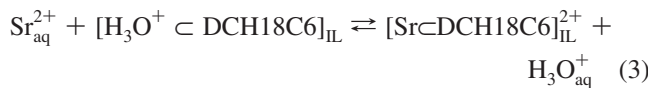
tant, D_{Sr} depends on the alkylation of imidazolium cation at N and C₂ positions: D_{Sr} decreases when the IL cation becomes more hydrophobic.¹⁶ Dietz et al.^{17,18} showed that the extraction mechanism toward 1-alkyl-3-methylimidazolium (C_nmim⁺)-based ILs depends on the size of the alkyl group: with n = 4, 5, extraction proceeds via a cation-exchange mechanism (eq 1) whereas for “bigger” and hence more hydrophobic imidazolium cations the mechanism is more like the one observed in conventional solvents where the nitrate counterions are coextracted with the strontium complex (eq 2).



However, according to EXAFS studies on the [C₁₀mim][Tf₂N] receiving phase (“classical mechanism”), the nitrates are not coordinated to the extracted Sr²⁺ (eq 2), in contrast to what is observed in a classical solvent like octanol.^{17,18} Regarding the IL, its anion X⁻ has also a striking effect on the extraction efficiency, via the IL’s cation exchange: the more hydrophobic X⁻, the highest the Sr²⁺ extraction by DCH18C6.¹⁹ There are cases where the hydrated proton H₃O⁺, present in acidic conditions^{4,17} or generated by radiolytic degradation of C_nmim⁺ ions²⁰ may display competitive complexation with the CE (eq 3), decreasing the D_{Sr} extraction coefficient. In other cases (e.g., Eu³⁺ extraction by diketonates)²¹ extraction to ILs proceeds via an anion exchange mechanism. As observed for the alkali cations extraction,²² the substituents and stereochemistry of the

* To whom correspondence should be addressed. E-mail: wipff@unistra.fr.

crown ether ligand also likely influence the partitioning of Sr²⁺ to IL.



The above-mentioned studies highlight the many chemical issues in using ILs in LLE processes, where small modifications may not only largely impact the extraction efficiency but also the underlying extraction mechanism. Hence a detailed microscopic knowledge of the distribution of the solutes in water–IL biphasic systems and of their solvation in the different solution domains, including the liquid–liquid interface, is required for an in-depth understanding of the driving forces in LLE with ILs.

This stimulated us to undertake molecular dynamics “MD” studies on the distribution of Sr²⁺ and its complexes with 18C6 at water/IL interfaces, comparing two ILs: [C₄mim][PF₆] and [C₈mim][PF₆] that are based on the same PF₆⁻ anion, and differ by the alkyl chains on imidazolium cations.²³ Both ILs make biphasic systems with water, but the latter is more hydrophobic.²⁴ Furthermore, as mentioned above, extraction to these liquids proceeds via different mechanisms. Several forms of the complexes are considered, depending on the status of the counterions: the charged [Sr_C18C6]²⁺ complex with dissociated nitrates and the neutral [Sr_C18C6,(NO₃)₂] complex with co-complexed nitrates. While the former is expected to form in a cation exchange process, the latter would be rather involved in a “classical” extraction process. Finally, in order to perform “apples to apples”²⁵ comparisons of the IL/water biphasic systems with classical analogues, we simulated with the same methodology neutral and charged Sr complexes at the water/chloroform interface, comparing 18C6 to DCH18C6 and a neutral to an acidic aqueous phase.

Methods

Force Field and Dynamics. The systems were simulated by classical molecular dynamics (MD) using the modified AMBER 7.0 software²⁶ in which the potential energy U is described by a sum of bond, angle, and dihedral deformation energies and pairwise additive 1-6-12 (electrostatic + van der Waals) interactions between nonbonded atoms.

$$U = \sum_{\text{bonds}} k_b(b - b_0)^2 + \sum_{\text{angles}} k_\theta(\theta - \theta_0)^2 + \sum_{\text{dihedrals}} \sum_n V_n(1 + \cos(n\phi - \gamma)) + \sum_{i < j} \left[\frac{q_i q_j}{R_{ij}} - 2\epsilon_{ij} \left(\frac{R_{ij}^*}{R_{ij}} \right)^6 + \epsilon_{ij} \left(\frac{R_{ij}^*}{R_{ij}} \right)^{12} \right]$$

Cross terms in van der Waals interactions were constructed using the Lorentz–Berthelot rules. The C₄mim⁺ ion parameters were taken from ref 27 while those of PF₆⁻ were from the OPLS force field²⁸ and have been tested on the pure liquid properties.^{29,30} The C₈mim⁺ parameters were derived from the C₄mim⁺ skeleton, to which a four-carbon chain with neutral atoms was added, as suggested by Liu et al.³¹ Atomic charges of the different IL ions were scaled by a factor of 0.9 to somewhat mimic the cation to anion charge transfer and better account for the miscibility of the IL with water.³² Water was described by the TIP3P model,³³ but tests with the SPCE model³⁴ have

also been performed. The van der Waals parameters for the Sr²⁺ and NO₃⁻ ions have been fitted on the free energies of hydration.^{35,36} The [Sr_C18C6]²⁺, [Sr_C18C6(NO₃)₂]⁺ and [Sr_C18C6(NO₃)₂]⁰ complexes were represented with ESP charges (see Figure S1 in the Supporting Information) fitted from ab initio DFT/B3LYP/6-31G* electrostatic potentials. Note that the resulting Sr charge ranges from ca. 1.47 to 1.18 e, thus somewhat reflecting the charge transfer from 18C6 and NO₃⁻ anion(s) to the cation, but formally reducing the Coulombic interactions between Sr, 18C6, and counterions (when cocomplexed). Thus, to retain a given coordination type for each complex at high temperature (400 K), we constrained Sr...O_{18C6} and Sr...O_{NO₃} distances at 2.65 and 2.75 Å, respectively, with harmonic force constants of 20 kcal·mol⁻¹ Å⁻². No constraints were applied at 300 K. The 1–4 van der Waals interactions were scaled down by a factor of 2.0 and 1–4 Coulombic interactions by a factor of 1.2, as recommended by Cornell et al.³⁷ The solutions were simulated using 3D-periodic boundary conditions, thus as alternating slabs of water and IL in the case of biphasic systems. Nonbonded interactions were calculated with a 12 Å atom based cutoff, and long-range electrostatic interactions were calculated using the Ewald summation method (PME, particle mesh Ewald approximation).³⁸

MD simulations were performed at constant temperature, coupling the system to a thermal bath using the Berendsen algorithm³⁹ with a relaxation time of 0.2 ps. All C–H and O–H bonds were constrained using SHAKE, while the Verlet leapfrog algorithm was used with a time step of 2 fs to integrate the equations of motion. The characteristics of the different simulated solutions are given in Table 1.

Monophasic Solutions. To simulate monophasic IL solutions, we first equilibrated “cubic” boxes of “dry” liquids containing 200 C_nmim⁺ PF₆⁻ ion pairs, yielding final densities (1.33 g·L⁻¹ for [C₄mim][PF₆] and 1.20 g·L⁻¹ for [C₈mim][PF₆]) in reasonable agreement with the experimental values (1.36 and 1.22 g·L⁻¹, respectively).⁴⁰ The “humid” [C₄mim][PF₆] liquid was constructed by adding 200 H₂O molecules to the “dry” liquid, thus with a 1:1 ratio of IL and water. This water content is higher than that reported for the pure IL, but may be more realistic in the presence of hydrophilic solutes like Sr²⁺.⁴¹ We then immersed each preformed [Sr_C18C6]²⁺, [Sr_C18C6(NO₃)₂]⁺ or [Sr_C18C6 (NO₃)₂]⁰ complex into the different ILs. For the first two complexes, the uncomplexed NO₃⁻ anions were placed at ca. 15 Å from the Sr atom. The systems were first equilibrated for 0.25 ns with fixed solutes (BELLY option of AMBER) followed by 0.25 ns at constant volume and 0.5 ns at constant pressure. We then performed 5 ns of dynamics at 400 K and at constant volume.

Biphasic Solutions. The liquid–liquid interface was built from adjacent “cubic” boxes of IL and water, and the solutes were immersed “at the interface” (see Figure S2 in the Supporting Information). Each system was then stepwise relaxed by (i) 1000 steps of steepest descent energy minimization, followed by (ii) 0.25 ns of dynamics with fixed solutes (BELLY option of AMBER) and (iii) 0.5 ns of dynamics at a constant pressure of 1 atm keeping the water molecules fixed (to obtain the correct density for the IL), and finally 0.5 ns of dynamics without constraints at a constant pressure of 1 atm. Final production runs were performed at a temperature of 300 K and at constant volume for 10–100 ns, depending on the system.

“Mixing–demixing” MD simulations were performed on solutions containing nine neutral or charged complexes (see Table 1 for details). After equilibration, the systems were first “randomly” mixed by running 2 ns of MD at 500 K with biased

TABLE 1: Characteristics of the Simulated Systems

	solute	solvent	box size (\AA^3)	time (ns)
IL Solutions				
	[Sr \subset 18C6] $^{2+}$ + 2 NO $_3^-$	200 C ₄ mim $^+$ PF ₆ $^-$	41.7 \times 41.7 \times 41.7	5
	[Sr \subset 18C6,(NO $_3$)] $^+$ + NO $_3^-$	200 C ₄ mim $^+$ PF ₆ $^-$	41.6 \times 41.6 \times 41.6	5
	[Sr \subset 18C6,(NO $_3$) $_2$]	200 C ₄ mim $^+$ PF ₆ $^-$	41.7 \times 41.7 \times 41.7	5
	[Sr \subset 18C6] $^{2+}$ + 2 NO $_3^-$	200 C ₄ mim $^+$ PF ₆ $^-$ + 200 H ₂ O	42.8 \times 42.8 \times 42.8	5
	[Sr \subset 18C6,(NO $_3$)] $^+$ + NO $_3^-$	200 C ₄ mim $^+$ PF ₆ $^-$ + 200 H ₂ O	42.8 \times 42.8 \times 42.8	5
	[Sr \subset 18C6,(NO $_3$) $_2$]	200 C ₄ mim $^+$ PF ₆ $^-$ + 200 H ₂ O	42.8 \times 42.8 \times 42.8	5
	[Sr \subset 18C6] $^{2+}$ + 2 NO $_3^-$	200 C ₈ mim $^+$ PF ₆ $^-$	45.6 \times 45.6 \times 45.6	5
	[Sr \subset 18C6,(NO $_3$)] $^+$ + NO $_3^-$	200 C ₈ mim $^+$ PF ₆ $^-$	45.7 \times 45.7 \times 45.7	5
	[Sr \subset 18C6,(NO $_3$) $_2$]	200 C ₈ mim $^+$ PF ₆ $^-$	45.6 \times 45.6 \times 45.6	5
Prebuilt IL-Water Interfaces				
A	27 Sr $^{2+}$ + 54 NO $_3^-$	467 C ₄ mim $^+$ PF ₆ $^-$ + 5400 H ₂ O	49.7 \times 49.7 \times 134.3	40
B _{TIP3P}	27 [Sr \subset 18C6] $^{2+}$ + 54 NO $_3^-$	365 C ₄ mim $^+$ PF ₆ $^-$ + 3552 H ₂ O	47.1 \times 47.1 \times 114.0	40
B _{SPCE}	27 [Sr \subset 18C6] $^{2+}$ + 54 NO $_3^-$	366 C ₄ mim $^+$ PF ₆ $^-$ + 3550 H ₂ O	47.0 \times 47.0 \times 113.7	80
C _{TIP3P}	27 [Sr \subset 18C6,(NO $_3$) $_2$]	363 C ₄ mim $^+$ PF ₆ $^-$ + 3554 H ₂ O	47.1 \times 47.1 \times 114.1	40
C _{SPCE}	27 [Sr \subset 18C6,(NO $_3$) $_2$]	363 C ₄ mim $^+$ PF ₆ $^-$ + 3548 H ₂ O	47.0 \times 47.0 \times 113.7	80
D	27 Sr $^{2+}$ + 54 NO $_3^-$	347 C ₈ mim $^+$ PF ₆ $^-$ + 5433 H ₂ O	49.6 \times 49.6 \times 134.1	40
E	27 [Sr \subset 18C6] $^{2+}$ + 54 NO $_3^-$	276 C ₈ mim $^+$ PF ₆ $^-$ + 3731 H ₂ O	47.3 \times 47.3 \times 114.5	80
F	27 [Sr \subset 18C6,(NO $_3$) $_2$]	267 C ₈ mim $^+$ PF ₆ $^-$ + 3817 H ₂ O	47.2 \times 47.2 \times 114.5	80
Mixing-Demixing				
G _{TIP3P}	9 [Sr \subset 18C6] $^{2+}$ + 18 NO $_3^-$	361 C ₄ mim $^+$ PF ₆ $^-$ + 4391 H ₂ O	44.7 \times 44.7 \times 134.2	70
G _{SPCE}	9 [Sr \subset 18C6] $^{2+}$ + 18 NO $_3^-$	361 C ₄ mim $^+$ PF ₆ $^-$ + 4391 H ₂ O (SPCE)	44.7 \times 44.7 \times 134.2	50
H _{TIP3P}	9 [Sr \subset 18C6,(NO $_3$) $_2$]	456 C ₄ mim $^+$ PF ₆ $^-$ + 3483 H ₂ O	45.1 \times 45.1 \times 135.3	85
H _{SPCE}	9 [Sr \subset 18C6,(NO $_3$) $_2$]	456 C ₄ mim $^+$ PF ₆ $^-$ + 3483 H ₂ O (SPCE)	45.1 \times 45.1 \times 135.3	100
I	9 [Sr \subset 18C6] $^{2+}$ + 18 NO $_3^-$	281 C ₈ mim $^+$ PF ₆ $^-$ + 4391 H ₂ O	44.8 \times 44.8 \times 134.6	50
J	9 [Sr \subset 18C6,(NO $_3$) $_2$]	281 C ₈ mim $^+$ PF ₆ $^-$ + 4391 H ₂ O	45.1 \times 45.1 \times 135.2	90
Chloroform-Water				
K	27 [Sr \subset 18C6] $^{2+}$ + 54 NO $_3^-$	936 MCl ₃ + 3750 H ₂ O	47.2 \times 47.2 \times 114.1	10
L	27 [Sr \subset 18C6,(NO $_3$) $_2$]	913 MCl ₃ + 3792 H ₂ O	47.1 \times 47.1 \times 114.0	10
M	27 [Sr \subset DCH18C6,(NO $_3$) $_2$]	936 MCl ₃ + 3750 H ₂ O	47.2 \times 47.2 \times 114.2	10
N	27 [Sr \subset DCH18C6,(NO $_3$) $_2$] 18 DCH18C6	1312 MCl ₃ + 4725 H ₂ O + 315 acid ^a	39.3 \times 39.3 \times 252.6	200

^a “acid” = HNO₃ + H₃O⁺ + NO₃⁻.

potentials (electrostatics scaled down by a factor 100). The subsequent “demixing simulation” was achieved by resetting the original electrostatics at a temperature of 300 K and running 50–100 ns of dynamics.

Analysis. The trajectories were analyzed by visual inspection at the computer graphics systems, and using our MDS software.⁴² Insights into energy components were obtained from the average interactions between selected groups (solute, IL, water). The average solvent distribution around a given solute was characterized by the radial distribution function (“RDF”) of the P_{PF₆}, F_{PF₆}, and N_{butyl} or N_{octyl} atoms.

The Z-position of the interface (Gibbs dividing surface) was dynamically calculated by the intersection of the water and IL density curves, defining the density of solvents and solutes (g·cm⁻³) by their mass per volume unit (d v = x·y·dz). We note, however, in contrast with classical “oil”/water interfaces,⁴³ the difficulty of precisely defining this position due to important IL/water mixing in some systems. As a result, the Z-position of Sr complexes was not sufficient to characterize, e.g., whether strontium is “extracted” or not. For this purpose, we examined at the computer graphics system the microenvironment of the complex and relationship with the bulk phases. In order to consistently compare different systems, we decided to define a same “interfacial domain” for all systems, within 7.5 Å from the Gibbs interface. According to solvent density curves, this distance corresponds to about half of the interfacial width, with marked modulations, though, depending on the system. Beyond 7.5 Å the solutes were considered to be in the “bulk” phases. Note that the simulated biphasic systems delineate two interfaces (noted ITF_A and ITF_B) and that solutes sometimes diffused from one interface to the other during the dynamics. The amount of

ions in a given domain was thus obtained from the nA + nB contributions.

Results

In the following, we first discuss the solvation of strontium complexes [Sr \subset 18C6,(NO $_3$) $_x$] $^{2-x}$ ($x = 0, 1$, or 2) in the “dry” [C₄mim][PF₆] and [C₈mim][PF₆] ILs, and in the “humid” [C₄mim][PF₆] liquid. We then describe the distribution of the [Sr \subset 18C6] $^{2+}$ and [Sr \subset 18C6,(NO $_3$) $_2$] complexes at preformed IL/water interfaces. Finally, we report the results of mixing–demixing simulations of water/IL mixtures containing either the charged or the neutral complexes. What happens at the classical chloroform/water interface is presented in the Discussion section.

1. Solvation of [Sr \subset 18C6,(NO $_3$) $_x$] Complexes ($x = 0, 1, 2$) in Monophasic [C₄mim][PF₆] and [C₈mim][PF₆] Solutions. In this section, we describe the solvation of the complexes in the phase where they are extracted, i.e., in the ionic liquids, comparing the two ILs and, for the more hygroscopic [C₄mim][PF₆], its “dry” vs “humid” states. Final snapshots of the C_nmim $^+$ and PF₆ $^-$ ions around the strontium complexes are given in Figure 1. The corresponding RDFs are given in Figure S3 (Supporting Information) and their characteristics are summarized in Table 2. In all cases, a given complex retained its initial coordination patterns during the dynamics, i.e., ranging from full dissociation of the nitrates from the [Sr \subset 18C6] $^{2+}$ complex to dicoordination of nitrates for [Sr \subset 18C6,(NO $_3$) $_2$], and monocoordination to [Sr \subset 18C6,(NO $_3$)] $^+$. Their solvation is discussed below.

[Sr \subset 18C6] $^{2+}$. In the “dry” [C₄mim][PF₆] and [C₈mim][PF₆] liquids, the complexed Sr $^{2+}$ ion rapidly coordinated to 2 PF₆ $^-$

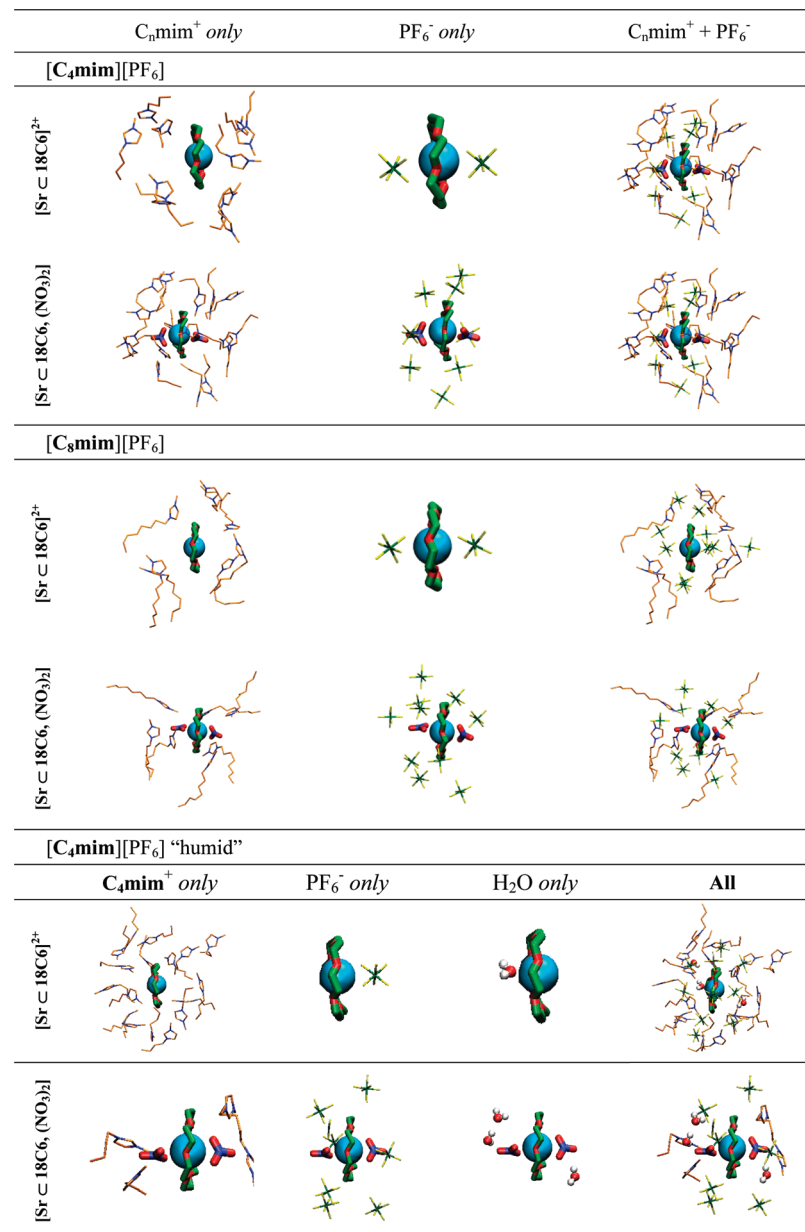


Figure 1. $[\text{Sr} \subset 18\text{C}6]^{2+}$ and $[\text{Sr} \subset 18\text{C}6, (\text{NO}_3)_2]$ complexes in “dry” ILs and in humid $[\text{C}_4\text{mim}][\text{PF}_6]$: typical snapshots of surrounding solvent species.

TABLE 2: Characteristics of the First Peak of the RDFs around Sr^{II} in IL Solutions: Integration Number (In Parentheses: Peak Maximum (\AA) and First Minimum (\AA))

	$\text{Sr}^{2+}-\text{P}_{\text{PF}_6}$	$\text{Sr}^{2+}-\text{F}_{\text{PF}_6}$	$\text{Sr}^{2+}-\text{N}_{\text{butyl}}$	$\text{Sr}^{2+}-\text{O}_{\text{H}_2\text{O}}$
		$[\text{C}_4\text{mim}][\text{PF}_6]$		
$[\text{Sr} \subset 18\text{C}6]^{2+} + 2 \text{NO}_3^-$	2.0 (3.7; 4.6)	4.3 (2.7; 3.6)	9.6 (7.4; 10.1)	
$[\text{Sr} \subset 18\text{C}6, (\text{NO}_3)_2]^+ + \text{NO}_3^-$	1.0 (3.8; 5.0)	2.0 (2.7; 3.6)	9.7 (6.8; 9.8)	
$[\text{Sr} \subset 18\text{C}6, (\text{NO}_3)_2]$	7.8 (7.8; 8.7)	24.0 (6.8; 7.9)	15.1 (7.4; 11.0)	
		$[\text{C}_4\text{mim}][\text{PF}_6][\text{H}_2\text{O}]$		
$[\text{Sr} \subset 18\text{C}6]^{2+} + 2 \text{NO}_3^-$	0.8 (4.2; 5.1)	1.1 (2.7; 3.6)	16.0 (9.3; 11.5)	2.0 (2.7; 3.7)
$[\text{Sr} \subset 18\text{C}6, (\text{NO}_3)_2]^+ + \text{NO}_3^-$	8.6 (7.6; 9.3)	30.1 (6.8; 8.0)	8.3 (8.0; 10.1)	1.1 (2.7; 3.5)
$[\text{Sr} \subset 18\text{C}6, (\text{NO}_3)_2]$	7.6 (7.8; 8.9)	21.0 (6.9; 7.7)	4.8 (6.4; 8.5)	1.0 (5.1; 5.5)
		$[\text{C}_8\text{mim}][\text{PF}_6]$		
$[\text{Sr} \subset 18\text{C}6]^{2+} + 2 \text{NO}_3^-$	2.0 (3.7; 4.5)	4.2 (2.7; 3.5)	6.6 (6.8; 9.9)	
$[\text{Sr} \subset 18\text{C}6, (\text{NO}_3)_2]^+ + \text{NO}_3^-$	1.0 (3.9; 5.0)	1.4 (2.7; 3.4)	6.0 (7.7; 9.3)	
$[\text{Sr} \subset 18\text{C}6, (\text{NO}_3)_2]$	12.1 (7.7; 10.5)	26.4 (6.8; 7.8)	8.7 (6.3; 9.9)	

anions (one at each face of the crown) that remained coordinated until the end of the dynamics (5 ns). According to the first peak of the $\text{Sr}-\text{F}_{\text{PF}_6}$ RDF, Sr is in contact with 4.3 F atoms at ca. 2.65 \AA on the average, indicating that each PF_6^- coordinates

mainly bidentate to Sr, with transient 3-coordinations during the dynamics. Beyond these anions, one finds a solvation shell comprising 10 C_4mim^+ or 7 C_8mim^+ cations and, respectively, 8 and 7 PF_6^- anions. These imidazolium cations are H-bonded

TABLE 3: Energy Analysis of $[\text{Sr} \subset 18\text{C}6, (\text{NO}_3)_n]^{2-n}$ Complexes in “Neat” ILs and in Chloroform: Intrasolute Energy (E_{COMP}^a), Solvent–Complex Interaction Energy ($E_{\text{SOL-IL}}$), Intra-IL Energy ($E_{\text{IL-IL}}^b$), and Total Energy E_{TOT} (in kcal/mol). Averages over the Last 1 ns

	E_{COMP}	$E_{\text{SOL-IL}}$	$E_{\text{IL-IL}}$	E_{TOT}
$[\text{Sr} \subset 18\text{C}6]^{2+} + 2 \text{NO}_3^-$	0	-453 (16)	-3753 (53)	-4206
	-199	-178 (9)	-3954 (56)	-4331
	-315	-95 (7)	-3944 (55)	-4354
$[\text{Sr} \subset 18\text{C}6, (\text{NO}_3)]^+ + \text{NO}_3^-$	0	[C ₄ mim][PF ₆]		
	-199	-349 (13)	-5425 (60)	-5801
	-315	-181 (11)	-5430 (51)	-5810
$[\text{Sr} \subset 18\text{C}6, (\text{NO}_3)_2]$	0	-108 (9)	-5394 (66)	-5817
	0	[C ₈ mim][PF ₆]		
	-199	-335 (11)	-1988 (65)	-2323
$[\text{Sr} \subset 18\text{C}6, (\text{NO}_3)_2]$	-199	-172 (14)	-1977 (64)	-2348
	-315	-101 (6)	-1969 (66)	-2385
	0	Chloroform		
$[\text{Sr} \subset 18\text{C}6]^{2+} + 2 \text{NO}_3^-$	0	-233 (8)	-3801 (16)	-4034
	-199	-111 (5)	-3926 (15)	-4236
	-315	-77 (4)	-3890 (15)	-4282

^a Relative to the dissociated complex. ^b Including dissociated nitrates.

to the F_{PF₆} atoms of the PF₆⁻ “ligands”, but not to the O_{18C6} oxygens of the crown (see RDFs in Figure S4).

In the “humid” [C₄mim][PF₆] liquid the Sr²⁺ solvation shell is more labile than in the “dry” liquid, as it involves an exchange between H₂O and PF₆⁻ ligands (Figure S5): 1 PF₆⁻ anion (mostly monodentate) and 2 H₂O molecules coordinate on the average to Sr during the last ns of dynamics.

[Sr₂C₆(NO₃)₂]⁺. From the beginning to the end of the dynamics, 1 PF₆⁻ anion coordinated to the Sr atom in both “dry” ILs, via 2 F atoms in the [C₄mim][PF₆] liquid and 1.4 F atoms in [C₈mim][PF₆], at average Sr–F distances of 2.7 Å, somewhat longer than in the [Sr₂C₆]²⁺ complex. In the “humid” IL, the solvent molecules around the [Sr₂C₆(NO₃)₂]⁺ complex are more mobile than in the “dry” [C₄mim][PF₆] liquid, as observed for the [Sr₂C₆]²⁺ complex: Sr²⁺ coordinates either 1 H₂O or 1 PF₆⁻ species along the dynamics.

[Sr₂C₆(NO₃)₂]. In the three simulated liquids the complexed Sr atom of that complex remains well shielded from solvent by 18C6 and the two nitrates. In the “dry” C₄mim⁺ and C₈mim⁺-containing ILs, the distal oxygens of the complexed nitrates are H-bonded to imidazolium ring protons, while in the “humid” IL they are solvated by H₂O molecules. The Sr–PF₆ RDF displays a first peak between 6 and 9 Å corresponding to ca. 25 PF₆⁻ anions that stabilize the first shell of C₄mim⁺ or C₈mim⁺ cations, leading to onion-type alternation of IL ions, as observed around alkali, alkaline earth, or lanthanide ions.^{44–46}

Energy Analysis of the Different Complexes. The results of an energy component analysis of the different systems are reported in Table 3. Because these systems have been simulated with identical numbers of solute species and IL ions, one can compare their total potential energies E_{TOT} as well as their components: $E_{\text{TOT}} = E_{\text{COMP}} + E_{\text{SOL-IL}} + E_{\text{IL-IL}}$, where E_{COMP} is the intracomplex energy calculated in the gas phase (from the QM optimizations at the DFT/B3LYP level using a 6-31+G basis set), $E_{\text{SOL-IL}}$ is the solute–IL interaction energy (“solvation energy”) and $E_{\text{IL-IL}}$ the internal energy of the ionic liquid. As expected, cocomplexation of nitrates stabilizes the solute (E_{COMP} becomes more negative), while its “solvation energy” $E_{\text{SOL-IL}}$ is significantly reduced in magnitude. The $E_{\text{IL-IL}}$ energy of the liquid itself also somewhat decreases. The net E_{TOT} energies of the different solutions indicate that [Sr₂C₆(NO₃)₂] with cocomplexed nitrates is the most stable form of complex in the ionic liquid solutions.⁴⁷ This is in good

accord with EXAFS data, showing that when the [Sr₂C₆(NO₃)₂] complex is solubilized into the [C₅mim][Tf₂N] ionic liquid, its two nitrates remain coordinated to Sr.⁴⁸ In the three liquids, the energy of the [Sr₂C₆(NO₃)₂]⁺ containing solution is intermediate between those of the solutions with 0 and 2 cocomplexed nitrates.

Looking at the “solvation energy” $E_{\text{SOL-IL}}$ of a given type of complex in C₄mim⁺ vs C₈mim⁺-based dry liquids, ones sees that the former liquid clearly better solvates the “dissociated” [Sr₂C₆]²⁺ species ($\Delta E_{\text{SOL-IL}} \approx 120$ kcal/mol), while the latter displays similar interactions with the charged and neutral complexes ($\Delta E_{\text{SOL-IL}} \approx 5$ kcal/mol). These features follow expected trends for a cation exchange mechanism with the [C₄mim][PF₆] IL. In the [C₈mim][PF₆] IL there is no clear-cut preference for a given type of complex.

2. Sr²⁺ and Its Complexes at Preformed IL–Water Interfaces. In this section, we analyze the distribution of Sr²⁺ uncomplexed and complexed at the preformed IL–water interfaces, i.e., starting from adjacent boxes of water and IL. The 27 solute species were initially placed on a 3 × 3 × 3 grid, i.e., nine at the interface ($Z \approx 0$) and the others on the aqueous side (9 at $Z \approx 20$ Å and 9 at $Z \approx 35$ Å; Figure S2, Supporting Information).

At the end of the dynamics, apart from a few exceptions where Sr is extracted to the bulk IL phase, complexes mainly partition between the interface and the bulk water, with marked modulations, however, depending on the nature of the IL and of the Sr complex (see Table 4 for the distribution of Sr²⁺ and NO₃⁻ species in the different systems). In the following, we will first briefly discuss the water–IL mixing in the different systems. We then successively describe the distribution and solvation of the “naked” Sr²⁺ cations (systems A and D), [Sr₂C₆]²⁺ complexes (systems B and E) and [Sr₂C₆(NO₃)₂] complexes (systems C and F) at both [C₄mim][PF₆] and [C₈mim][PF₆] interfaces. The final snapshots of the solvent boxes and average solvent density curves are given in Figure 2 (systems A–C with the [C₄mim][PF₆] IL) and Figure 3 (systems D–F with the [C₈mim][PF₆] IL). Unless otherwise specified, the results correspond to the TIP3P water model.

2.1. Water–IL Mixing. As observed at the neat IL/water interfaces,^{32,49,50} one finds H₂O molecules in the IL phase and IL ions in the water phase (see details in Table 5), with a marked

TABLE 4: Prebuilt Interfaces (Systems A–F). Average Number of Sr^{2+} and NO_3^- Species in the Different Domains: “at the Interface” (Within 7.5 Å from the Gibbs Surface), in “Bulk Water” and in Bulk IL”, and Averages over the Last 5 ns of Dynamics

		bulk IL	interface _A	bulk H ₂ O	interface _B
A	Sr^{2+}	0.0 (0.2)	2.7 (1.4)	21.2 (1.3)	2.5 (1.1)
	NO_3^-	0.2 (0.5)	4.7 (1.9)	42.7 (2.7)	5.4 (1.7)
B_{TIP3P}	Sr^{2+}	2.3 (0.5)	4.6 (0.9)	15.7 (1.3)	4.4 (1.0)
	NO_3^-	1.2 (0.9)	8.8 (2.5)	36.5 (2.6)	7.5 (1.7)
B_{SPCE}	Sr^{2+}	1.1 (0.4)	7.2 (0.8)	14.6 (1.1)	4.1 (0.9)
	NO_3^-	0.0 (0.1)	8.5 (1.5)	36.5 (2.0)	9.0 (2.1)
C_{TIP3P}	Sr^{2+}	5.8 (1.2)	8.6 (1.4)	7.8 (1.2)	4.8 (0.9)
C_{SPCE}	Sr^{2+}	1.1 (0.8)	12.6 (0.9)	8.7 (1.2)	4.6 (0.7)
D	Sr^{2+}	0.0 (0.0)	1.8 (1.1)	24.0 (1.4)	1.2 (0.9)
	NO_3^-	0.0 (0.1)	7.1 (2.0)	41.5 (2.6)	5.2 (1.8)
E	Sr^{2+}	0.0 (0.1)	2.1 (1.0)	19.3 (1.2)	5.6 (1.2)
	NO_3^-	0.3 (0.6)	7.7 (2.0)	35.3 (2.6)	10.7 (1.8)
F	Sr^{2+}	0.0 (0.1)	8.9 (1.1)	13.0 (1.3)	5.1 (0.6)

dependence on the water model. In the different systems, the molar fraction of water x_{Wat} in the IL phase is found to be about 2.5 times higher with the TIP3P than with the SPCE model (0.64 for B_{TIP3P} vs 0.27 for B_{SPCE} , and 0.73 for C_{TIP3P} vs 0.30 for C_{SPCE}). These values are comparable to those obtained for the corresponding neat interfaces.⁵⁰ The nature of the IL phase also strongly influences the amount of extracted water: the more “hydrophobic” $[\text{C}_8\text{mim}][\text{PF}_6]$ IL extracts ca. 30% less water than $[\text{C}_4\text{mim}][\text{PF}_6]$: $x_{\text{Wat}} = 0.44$ for system E ($[\text{Sr} \subset 18\text{C}6]^{2+}$) and 0.39 for system F ($[\text{Sr} \subset 18\text{C}6, (\text{NO}_3)_2]$). These results agree well with those obtained from simulations³² and follow experimental trends on the neat ILs humidity.²⁴

On the other side, IL ions are extracted to the bulk aqueous phase, by a larger amount with the TIP3P water model than

with the SPCE model. Interestingly, with both water models, the nature of the strontium complexes influences the amount of IL ions dissolved in bulk water. While in the presence of $[\text{Sr} \subset 18\text{C}6]^{2+}$ complexes, C_4mim^+ cations are in excess over PF_6^- anions in water (37 C_4mim^+ vs 31 PF_6^- for system B_{TIP3P} , 16 C_4mim^+ vs 9 PF_6^- for B_{SPCE}), in the presence of neutral $[\text{Sr} \subset 18\text{C}6, (\text{NO}_3)_2]$ complexes the numbers of C_4mim^+ and PF_6^- ions in water are nearly identical (18 and 19, respectively for system C_{TIP3P} , 12 and 11, respectively for C_{SPCE}).

Comparing now the different solutions with the more hydrophobic $[\text{C}_8\text{mim}][\text{PF}_6]$ IL, one sees that their bulk water domain contains much less IL ions than with the $[\text{C}_4\text{mim}][\text{PF}_6]$ IL. In systems E and F, one finds only 8 and 4 PF_6^- ions, respectively, and only 0–1 C_8mim^+ ion in bulk water, thus making a cation exchange mechanism highly improbable with the most hydrophobic IL. Note that these distributions follow expected trends in the case of a cation exchange mechanism with the $[\text{C}_4\text{mim}][\text{PF}_6]$ IL and of a classical mechanism with the $[\text{C}_8\text{mim}][\text{PF}_6]$ IL.

2.2. Naked Sr^{2+} Cations at the Aqueous Interfaces with the $[\text{C}_4\text{mim}][\text{PF}_6]$ and $[\text{C}_8\text{mim}][\text{PF}_6]$ Liquids. As expected, in the absence of crown ether, the majority of the 27 Sr^{2+} ions sit in bulk water. In the interfacial domains A and B, one finds on the average (over the last 5 ns) 5.2 Sr^{2+} (2.7 at ITF_A and 2.5 at ITF_B) with the $[\text{C}_4\text{mim}][\text{PF}_6]$ liquid, and only 3.0 Sr^{2+} (1.8 at ITF_A and 1.2 at ITF_B) with the $[\text{C}_8\text{mim}][\text{PF}_6]$ liquid. In all cases Sr^{2+} is fully hydrated by about 8 H_2O molecules, while PF_6^- anions sit in the second shell or beyond. Sr^{2+} cations diffuse rapidly and exchange between the bulk and the interfacial water domains. The residence time of Sr^{2+} at the interface is found to be rather short (ca. 35 ps). Regarding the nitrate counterions in the interfacial domain, they are ca. twice more concentrated than Sr^{2+} cations: there are 10.1 nitrates (4.7 at ITF_A and 5.4 at ITF_B)

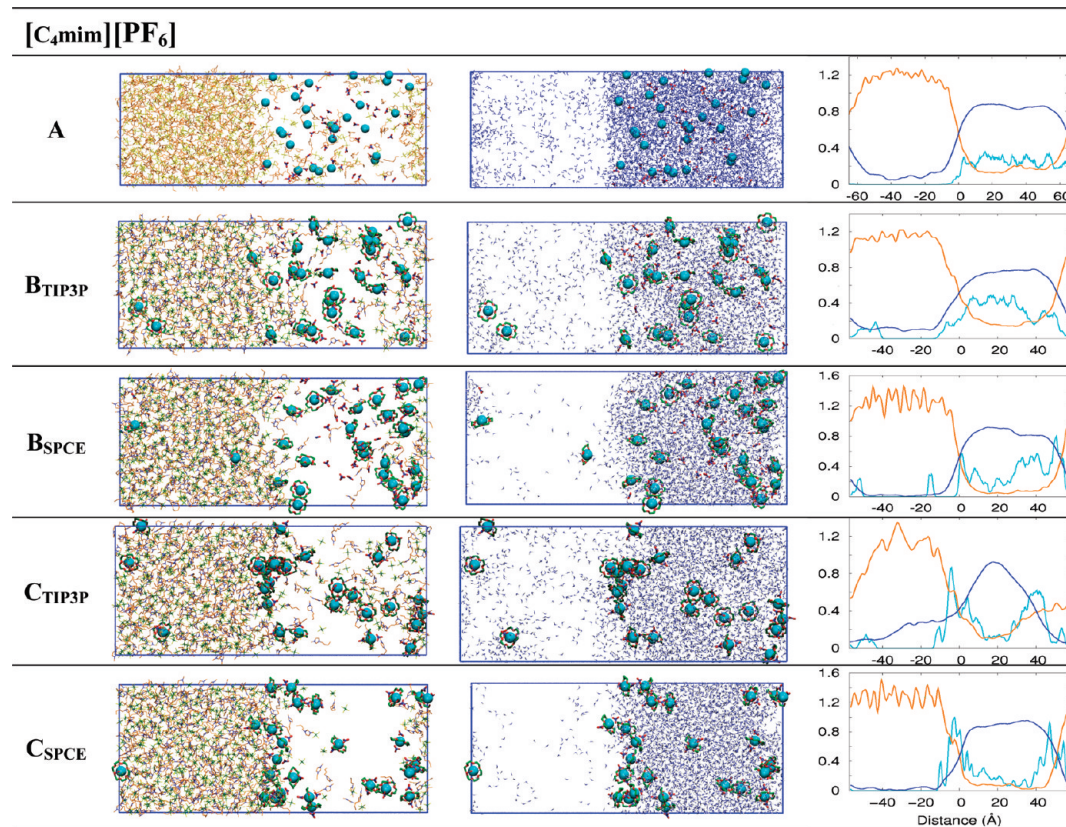


Figure 2. Systems A–C in $[\text{C}_4\text{mim}][\text{PF}_6]$ /water solutions. Final snapshots of the simulation box (left). The two liquids are represented side by side for clarity. Average density curves over the last 5 ns of dynamics (right) for water (blue), IL (orange), and Sr (cyan).

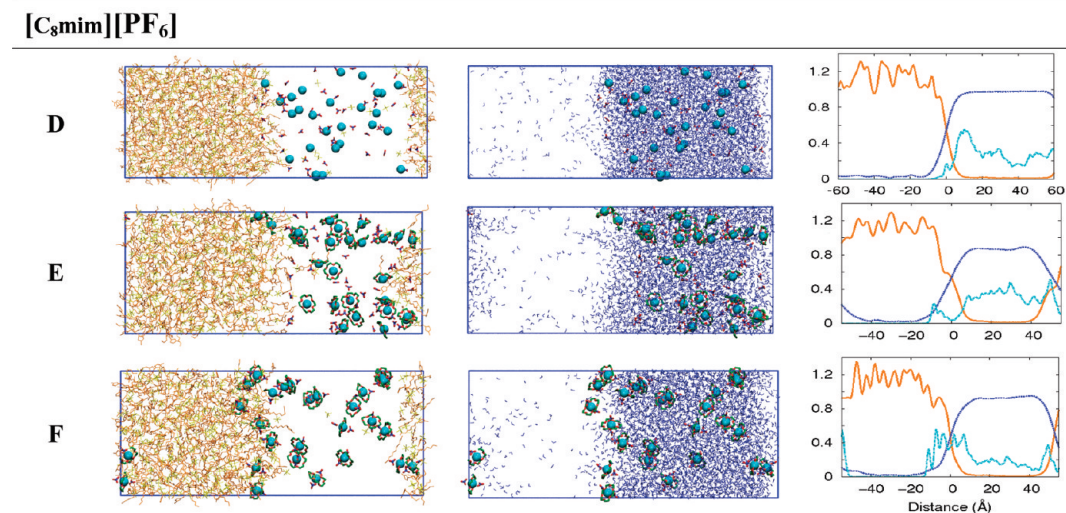


Figure 3. Systems D–F in $[C_8\text{mim}][\text{PF}_6]$ /water solutions: final snapshots of the simulation box (left) with the two liquids represented side by side for clarity. Average density curves over the last 5 ns of dynamics (right) for water (blue), IL (orange), and Sr (cyan).

with the $[C_4\text{mim}][\text{PF}_6]$ liquid, and 12.3 nitrates (7.1 at ITF_A and 5.2 at ITF_B) with the $[C_8\text{mim}][\text{PF}_6]$ liquid.

2.3. $[\text{Sr} \subset 18\text{C}6]^{2+}$ at the Aqueous Interfaces with the $[C_4\text{mim}][\text{PF}_6]$ and $[C_8\text{mim}][\text{PF}_6]$ Liquids. To study the biphasic $[C_4\text{mim}][\text{PF}_6]$ /water solutions with the charged $[\text{Sr} \subset 18\text{C}6]^{2+}$ complexes, we compared the TIP3P and SPCE water models (systems B_{TIP3P} and B_{SPCE}). Interestingly, with both models, one observes some extraction of $[\text{Sr} \subset 18\text{C}6]^{2+}$ complexes (2 in B_{TIP3P} and 1 in B_{SPCE}), as described hereafter (see Figure 4).

In the B_{TIP3P} simulation, the first complex, initially in water, diffuses to the interface in ca. 20 ns, and then slowly migrates into the IL phase, up to a maximum distance of 27 Å from the interface until the end of the dynamics. The second “extracted” complex, also initially in water, has a more irregular dynamics. It first diffuses to the interface in ca. 25 ns, and further away toward the IL, up to distance of 17 Å from the interface after ca. 10 ns. Later on, it oscillates between the interface and the IL phase, with a lifetime of ca. 3 ns in each region. In the B_{SPCE} simulation with the SPCE model, one also observes the “extraction” of a complex (Figure 4), less pronounced, however, than with the TIP3P water model. Indeed, that complex initially at the interface oscillates between the IL side and the water side of the interface for ca. 50 ns, and later on migrates toward the IL phase, up to ca. 15 Å from the interface at the end of the dynamics.

In both B_{TIP3P} and B_{SPCE} systems, the extracted complex(es) have similar solvation features (see Figure 4). The complexed Sr ion is coordinated to 3 water molecules, without any connection (e.g., “water finger”)⁵¹ to the bulk water phase. The second Sr shell comprises a mix of 4–7 H_2O and 2–3 PF_6^- species. Regarding the NO_3^- counterions, none is coextracted to the IL phase in the B_{SPCE} system, whereas in the B_{TIP3P} system, 1–2 are coextracted, uncoordinated to the Sr^{2+} cation.

The majority of the remaining charged complexes (25–26) dynamically exchange between the interfacial and bulk aqueous domains. On the average, with both water models, there are ca. 15 complexes in bulk water (15.7 in TIP3P water and 14.6 in SPCE water) and a significant amount in the interfacial domains: 9.0 (4.6 at ITF_A and 4.4 at ITF_B) in the B_{TIP3P} solution and 11.3 (7.2 at ITF_A and 4.1 at ITF_B) in the B_{SPCE} solution. Note that this amount is nearly twice that observed for the “naked” Sr^{2+} cations, showing the importance of Sr^{2+} complexation by 18C6 ligands to approach the interface. In the interfacial domain, with both water models, the majority of the charged complexes sit on the water side (75% in B_{TIP3P} and 57% in B_{SPCE}), pointing to stronger interactions with the aqueous than with the IL phase. Indeed, these complexes are mainly surrounded by water molecules, and by only 0.25 PF_6^- anions, on the average. Regarding the total nitrate charges in the interfacial domain (ca. −16.3 e for B_{TIP3P} and −17.5 e for B_{SPCE}), it is somewhat lower than the positive charge of Sr^{2+} cations (18 e for B_{TIP3P} and 22.6 e for B_{SPCE}). As result, in the bulk aqueous phase, NO_3^- charges are somewhat in excess over the Sr^{2+} charges, in keeping with the excess of $C_4\text{mim}^+$ cations over PF_6^- anions.

In the case of system E with the $[C_8\text{mim}][\text{PF}_6]$ ionic liquid, no charged $[\text{Sr} \subset 18\text{C}6]^{2+}$ complex is extracted during the dynamics. The complexes partition between the bulk aqueous and interfacial domains. In the latter, there are slightly less complexes (7.7) than in system B_{TIP3P} with the $[C_4\text{mim}][\text{PF}_6]$ IL (9.0), leading to a somewhat higher concentration in the aqueous phase with the more hydrophobic IL. As above, complexes at the interface are mainly solvated by water, and by only 0.05 PF_6^- anions.

Statistical averages hide an interesting extraction event that occurred during the dynamics of system E (see Figure 5): one of the complexes initially in the aqueous phase first diffused to

TABLE 5: Prebuilt Interfaces (Systems A–F). Average Number of Water Molecules in the IL Phase and $C_n\text{mim}^+$ or PF_6^- Ions in the Aqueous Phase, and Averages over the Last 5 ns of Dynamics

A	B_{TIP3P}	B_{SPCE}	C_{TIP3P}	C_{SPCE}	D	E	F
483 (34)	481 (3)	103 (9)	785 (24)	115 (12)	128 (10)	163 (15)	134 (8)
			$H_2\text{O}$ Molecules in IL Phase				
45 (2)	37 (3)	16 (2)	18 (3)	12 (2)	1 (1)	2 (1)	1 (1)
44 (3)	31 (3)	9 (2)	19 (3)	11 (2)	8 (2)	8 (1)	4 (1)
			$C_n\text{mim}^+$ + PF_6^- Ions in the Aqueous Phase				

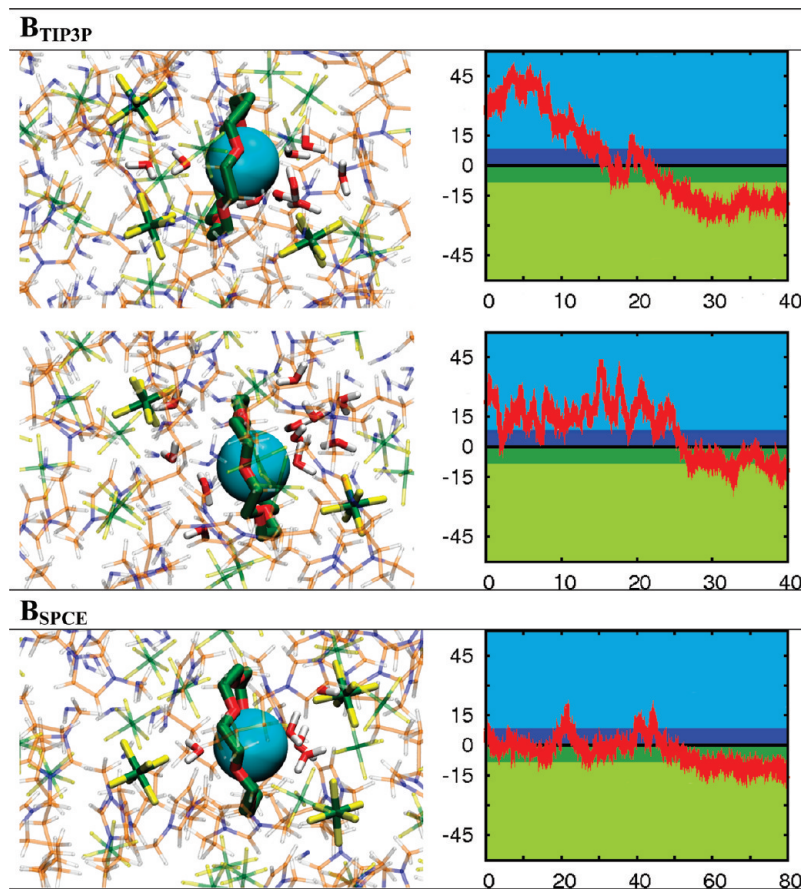


Figure 4. Zoomed views on the extracted charged complexes in systems B_{TIP3P} and B_{SPC-E} and Z-distance (Å) of the complexes from the interface ($Z = 0$) along the dynamics (time in ns). Water side in blue and IL side in green.

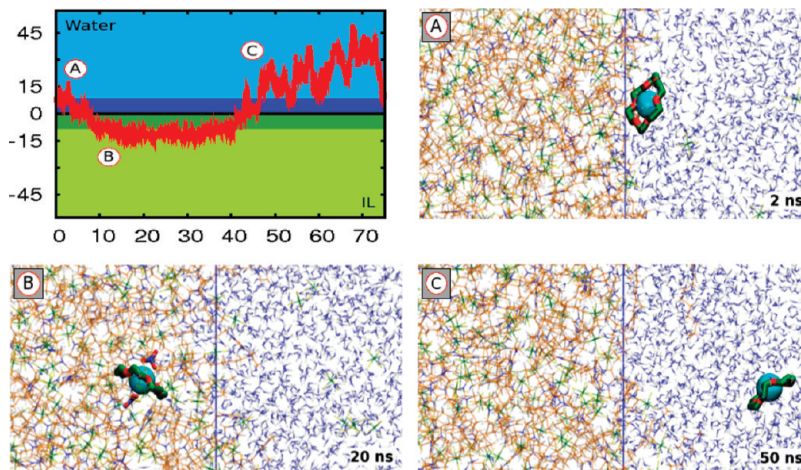


Figure 5. Sr complex “extracted” at the [C₈mim][PF₆]/Water interface (system E): Z distance of Sr from the interface ($Z = 0$) along the trajectory (top left) and snapshots during the dynamics. Other solutes are omitted for clarity.

the water side of the interfacial domain, where it successively complexed two nitrates to form the neutral [Sr \subset 18C6(NO₃)₂] species. The latter then migrated to the IL phase, up to ca. 10 Å where it remained for about 10 ns. Later on, the two NO₃⁻ dissociated, presumably because of underestimated attractions in this model⁵² and moved back to the bulk aqueous phase. Extraction to the [C₈mim][PF₆] liquid via the neutral [Sr \subset 18C6(NO₃)₂] complex is consistent with a classical extraction mechanism, with cocomplexed nitrates, though.

2.4. Neutral [Sr \subset 18C6,(NO₃)₂] Complexes at the Aqueous Interfaces with the [C₄mim][PF₆] and [C₈mim][PF₆] Liquids. As for the charged complexes, we simulated 27 neutral [Sr \subset 18C6,(NO₃)₂] complexes at the [C₄mim][PF₆]/water inter-

face. With both water models (systems C_{TIP3P} and C_{SPC-E}), extraction of complexes occurred during the dynamics. With the TIP3P model, one finds 5.8 complexes on the IL side, beyond 7.5 Å from the Gibbs interface. These are formally in the IL domain, but only two no longer have water connections with the interface and are really extracted. In fact, the first one leaves the interface after 25 ns and then slowly diffuses to the bulk IL, up ca. 28 Å from the interface. Likewise, the second complex quits the interfacial domain after 35 ns and further moves to the bulk IL domain at a distance of 22 Å (Figure 6). The other four complexes beyond 7.5 Å from the interface retain water connections with the interfacial water along the dynamics and thus cannot be considered as extracted.

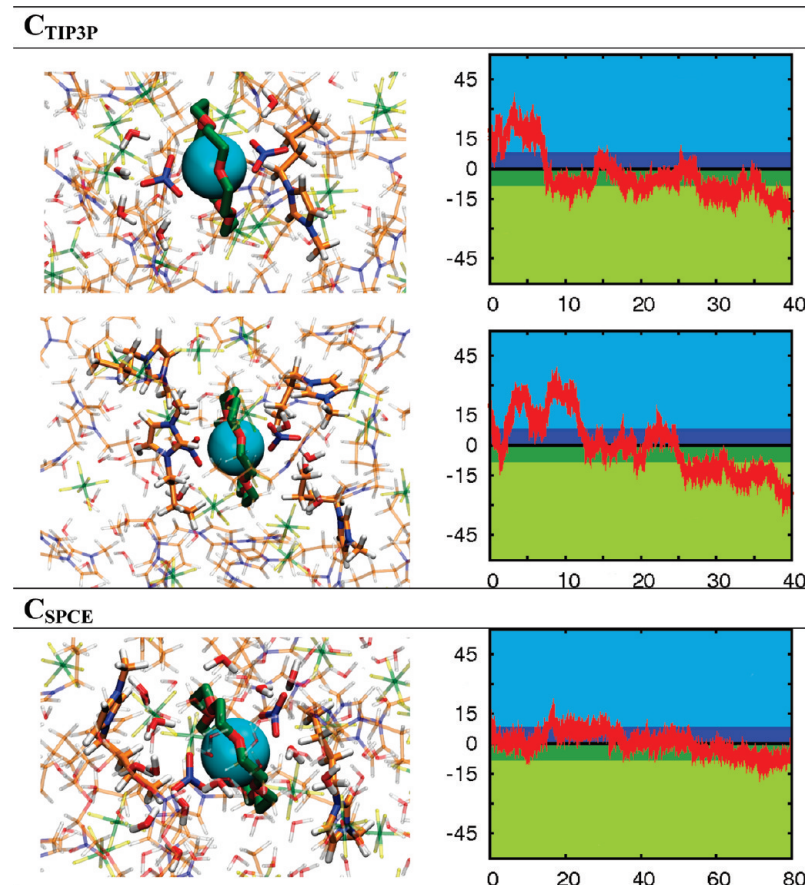


Figure 6. Zoomed views on the extracted neutral complexes in systems C_{TIP3P} and C_{SPCE} and Z distance (Å) of the complexes from the interface along the dynamics (time in ns). Water side in blue and IL side in green.

With the SPCE model (system C_{SPCE}) one also observes the extraction of a [Sr_C18C6,(NO₃)₂] complex (see Figure 6), after ca. 25 ns. It does however, not migrate further into the bulk IL, and remains within 6–17 Å from the interface.

The solvation patterns of the “extracted” neutral complexes in C_{TIP3P} and C_{SPCE} systems are quite similar (see Figure 6). Since Sr is shielded by the nitrates and the crown, it neither coordinates IL anions nor water. Water molecules and C₄mim⁺ cations in fact solvate the complexed nitrates, forming H-bonds with their distal oxygens (Figure 6). The crown itself is mainly surrounded by IL ions.

Looking at the [Sr_C18C6,(NO₃)₂] complexes in the bulk aqueous phase, their number (7.8 and 8.7, respectively, in the C_{TIP3P} and C_{SPCE} solutions) is about half the number of charged [Sr_C18C6]²⁺ complexes in the B_{TIP3P} and B_{SPCE} solutions. Conversely, in the interfacial domain, there are more neutral than charged complexes. Furthermore, a significant amount of neutral complexes (60% in C_{TIP3P} and 40% in C_{SPCE}) sits on the IL side of the interface. Their nitrate ligands are H-bonded to water molecules and, occasionally, to ring protons of C₄mim⁺ IL ions. Their crown ether moiety is surrounded by a “random” mixture of water molecules and IL ions.

With the more hydrophobic [C₈mim][PF₆] liquid (F system), one observes no clear strontium extraction. Furthermore, there are less complexes in the interfacial domains (8.9 at ITF_A and 5.1 at ITF_B) than with the [C₄mim][PF₆] IL. This is more, however, than for the charged complexes, confirming that neutral complexes are more “surface active” than the charged ones. In the interfacial domain, neutral complexes are nearly equally shared between the IL side and the water side of the interface. They are mainly solvated by 3–4 water molecules H-bonded

to the NO₃⁻ ligands and, for those sitting on the IL side of the interface, by a C₄mim⁺ cation interacting sometimes with NO₃⁻ anions. As in the C_{TIP3P} system, the crown ether part of the complexes at the interface is mostly surrounded by a mixture of both liquids, without specific interactions.

3. Mixing–Demixing Simulations. In order to test to which extent the distributions obtained at preformed interfaces depend on the initial state, we decided to undertake a series of mixing–demixing simulations on solutions containing nine complexes, again comparing their [Sr_C18C6]²⁺ to [Sr_C18C6,(NO₃)₂] forms, and [C₄mim][PF₆] to [C₈mim][PF₆] as ionic liquids. The demixing simulations were run for 50–100 ns of dynamics (see Table 1). The final views of these systems (Figure 7) show that, in spite of the long simulated times, the final states markedly differ from those obtained from juxtaposed phases. As observed for neat water/IL mixtures,⁵⁰ the water and IL phases are less well separated than in simulations that started with juxtaposed liquids.

This is particularly the case for the [C₄mim][PF₆]/water systems G and H with the most hygroscopic IL and with TIP3P water. With the SPCE water model, however, a more visible separation of different domains appears, but some H₂O molecules remained in the IL-rich phase and some IL cations and anions remained in the aqueous domain. Interestingly, one can see that 3–4 [Sr_C18C6]²⁺ complexes (system G_{SPCE}) and 2 [Sr_C18C6,(NO₃)₂] complexes (system H_{SPCE}) remain locally surrounded by IL molecules, and can thus be considered as “extracted”. The remaining 4–5 [Sr_C18C6]²⁺ species (system G_{SPCE}) are mainly surrounded by “bulk” water while the remaining 7 [Sr_C18C6,(NO₃)₂] neutral complexes (system H_{SPCE}) rather concentrate in the interfacial regions.

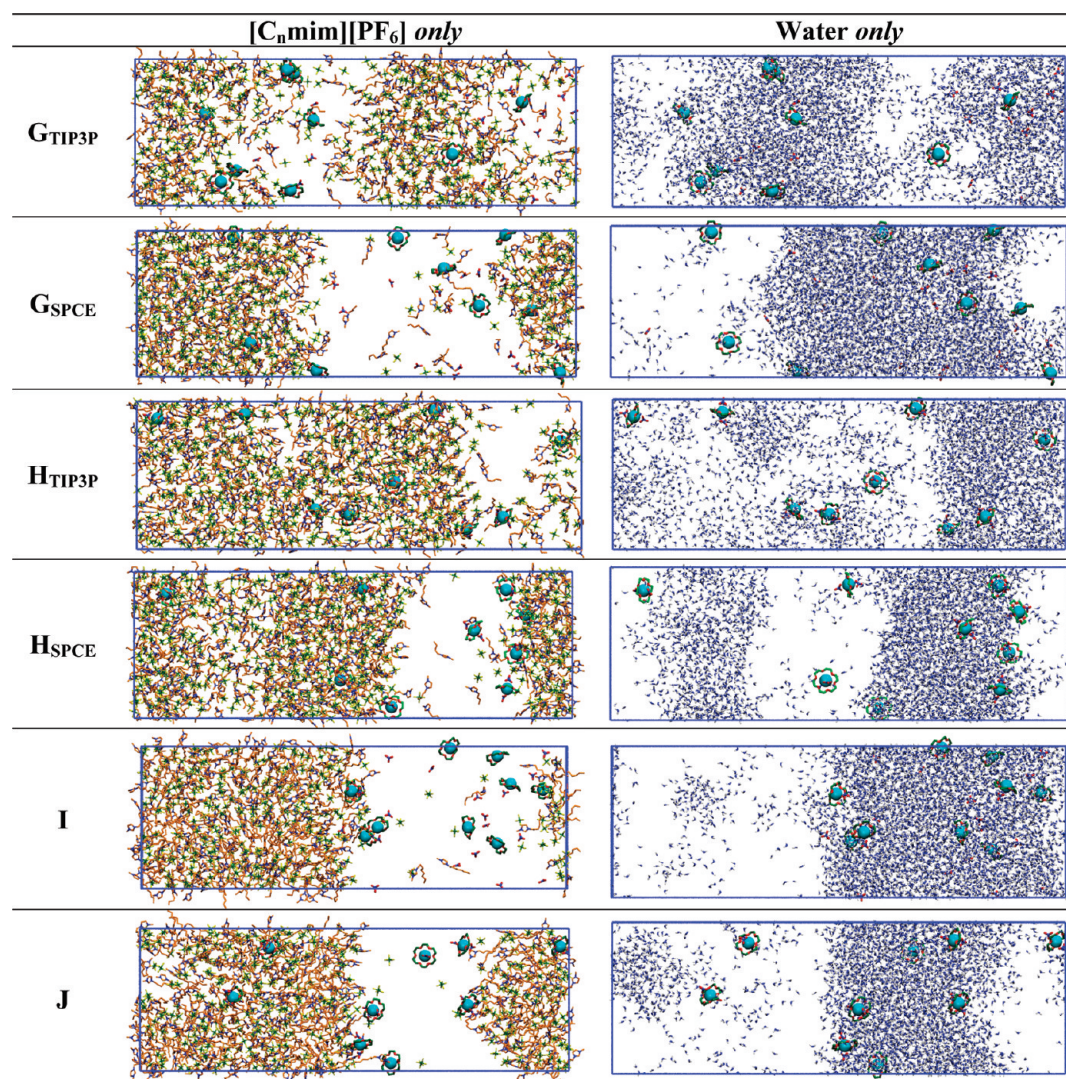


Figure 7. Demixing simulations of IL/water mixtures with nine Sr complexes. Solvents shown side by side instead of superposed for clarity. The IL is either $[C_4mim][PF_6]$ (systems G and H) or $[C_8mim][PF_6]$ (systems I and J). Complexes are either charged (systems G and I) or neutral (systems H and J). The initial mixed states (0 ns) are shown in Figure S6 in the Supporting Information.

For systems I and J based on the hydrophobic $[C_8mim][PF_6]$ liquid, one observes a better, but still incomplete phase separation. In the J system with $[Sr\subset 18C6, (NO_3)_2]$ complexes, 3 complexes finally sit in the IL phase and the 6 others concentrate at the interface. In the I system with the charged $[Sr\subset 18C6]^{2+}$ complexes, none is extracted to the IL. About 6 complexes prefer the bulk aqueous phase, but ca. 3 are close to the interface.

To summarize, the demixing simulations that started with artificially mixed liquids, although not yielding full phase separation at the simulated times, provide similar qualitative features about the effect of the IL nature and state of the counterions: cocomplexation of nitrates renders the complex less hydrophilic and more surface active. Furthermore, there is more extraction of neutral complexes to the most hydrophobic $[C_8mim][PF_6]$ liquid, and of charged complexes to the $[C_4mim][PF_6]$ liquid.

Discussion and Conclusion

On the basis of MD simulations, we have investigated interfacial systems possibly involved in the strontium extraction

by crown ethers to two ionic liquids, $[C_4mim][PF_6]$ and $[C_8mim][PF_6]$, where extraction proceeds much more efficiently than toward classical organic solvents, and with different extraction mechanisms. Throughout the study, we consistently compared two forms of the complex, namely the neutral form $[Sr\subset 18C6, (NO_3)_2]$ with cocomplexed nitrates and the charged form $[Sr\subset 18C6]^{2+}$ with dissociated nitrates, respectively, involved in different extraction mechanisms.

Solvation in the “Oil” Phase. According to an energy analysis on monophasic $[C_4mim][PF_6]$ and $[C_8mim][PF_6]$ solutions, those containing the neutral $[Sr\subset 18C6, (NO_3)_2]$ complex are more stable than those containing the charged $[Sr\subset 18C6]^{2+}$ and $[Sr\subset 18C6, (NO_3)]^+$ complexes with dissociated nitrate(s). This is in good agreement with EXAFS results.⁴⁸ Furthermore, comparing “solvation energies” in the two ionic liquids and in chloroform (Table 3) makes clear that each type of complex is better solvated in the former environment, contributing to the higher extraction efficiency to ionic liquids. In fact, the IL affords polar moieties that better solvate the complex than does, e.g., chloroform: while PF_6^- can coordinate to the Sr cation of the charged complexes, C_4mim^+ or C_8mim^+ cations solvate the

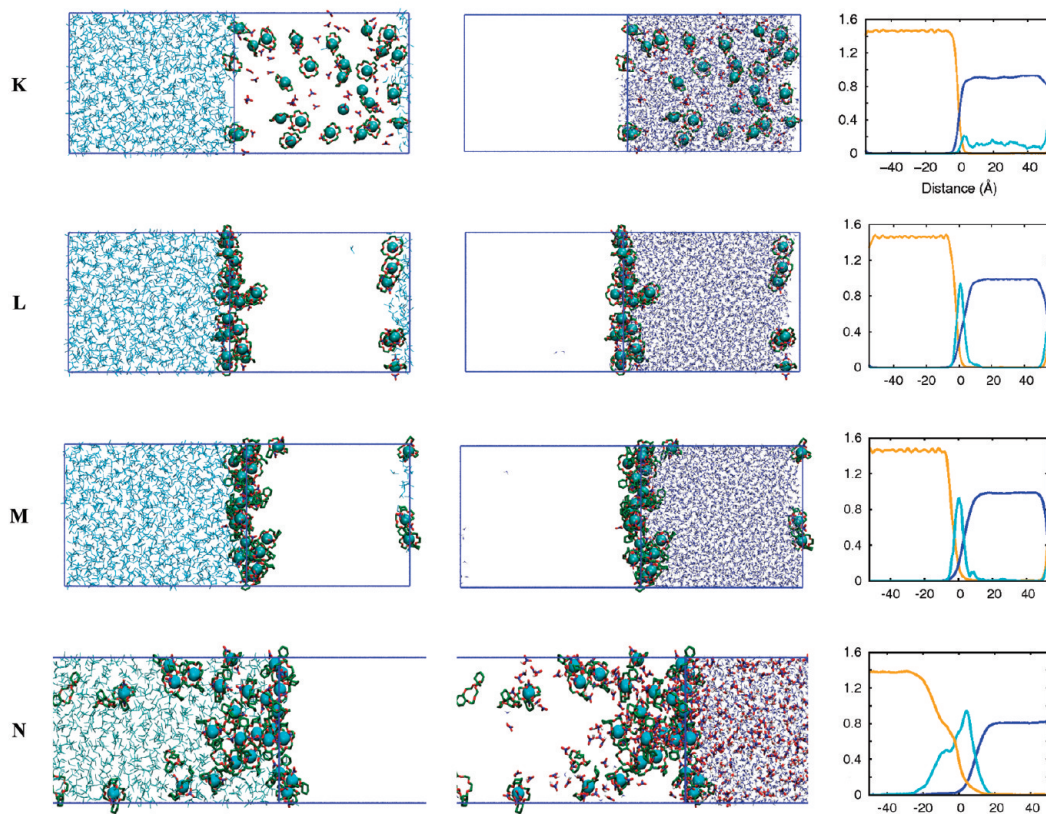
CHLOROFORM

Figure 8. Chloroform–water interface: final snapshots of the simulation box (left) with the two liquids represented side by side for clarity. Average density curves over the last 2 ns of dynamics (right). From top to bottom: systems K with the charged $[\text{SrC}18\text{C}_6]^{2+}$ complexes and L with the neutral $[\text{SrC}18\text{C}_6(\text{NO}_3)_2]$ complexes, system M with the $[\text{SrCDCH}18\text{C}_6(\text{NO}_3)_2]$ complexes, and system N with $[\text{SrCDCH}18\text{C}_6(\text{NO}_3)_2]$ complexes, free DCH18C6 ligands, and acidic water.

nitrates counterions (either cocomplexed or “free”). Furthermore, water solubilized in hygroscopic ILs like $[\text{C}_4\text{mim}][\text{PF}_6]$ solvates the polar groups of the complex, better than would do chloroform.

Complexes at a Classical Aqueous (Nano)interface. What happens at the interface is of utmost importance in liquid–liquid extraction.⁵³ Before discussing these IL/water biphasic systems, it is worth describing as a reference the classical chloroform/water solutions containing the same solutes in similar concentrations (systems K with the charged $[\text{SrC}18\text{C}_6]^{2+}$ complexes and L with the neutral $[\text{SrC}18\text{C}_6(\text{NO}_3)_2]$ complexes). These are compared to the $[\text{SrCDCH}18\text{C}_6(\text{NO}_3)_2]$ complexes formed with the more hydrophobic DCH18C6 ligands (system M). Final snapshots in Figure 8 make clear that charged $[\text{SrC}18\text{C}_6]^{2+}$ complexes mainly partition in the aqueous phase that strongly solvates the complexed Sr^{2+} and the dissociated NO_3^- species.⁵⁴ They can thus hardly be extracted as such. Classical extraction requires charge neutralization by counterions. Indeed, all neutral $[\text{SrC}18\text{C}_6(\text{NO}_3)_2]$ complexes (system L) or $[\text{SrCDCH}18\text{C}_6(\text{NO}_3)_2]$ complexes (system M) are expelled out of the bulk water phase at the beginning of the dynamics, but none diffuse to the organic phase. As observed for neutral extractants,^{55–58} they all adsorb at the interface(s) (20 at ITF_A and 7 at ITF_B in system L; 24 at ITF_A and 3 at ITF_B in system M). The main reason is their stronger attraction energy with water than with chloroform at the interface.⁵⁹ As shown by experiments, crown ethers,⁶⁰ neutral extractant molecules,^{61,62} and their complexes are surface active. During the macroscopic phase separation, diffusion from

the interface to the “oil phase” can be promoted upon reduction of the interfacial area (e.g., by collapse of water-in-oil droplets formed upon agitation of the liquids) and/or after saturation of the interface (by ligands and their complexes).^{63,64}

Complexes at IL–Aqueous (Nano)interfaces. The simulated IL/water biphasic strontium solutions differ from the chloroform/water analogues by a number of features. First, as for neat interfaces,⁵⁰ note the difficulty of equilibrating the IL biphasic systems. In spite of our computational efforts, simulations that started from juxtaposed liquids did not converge to the same separated phases, compared to those obtained from artificially mixed liquids (mixing–demixing simulations), due to the viscosity of the IL, the slow diffusion of its components, and to the stronger interactions of the IL with water, compared to classical organic molecules. We thus in the following mainly discuss features observed for juxtaposed liquids.

Interfacial landscapes with ILs differ from those of classical aqueous–oil interfaces that are thin (ca. 1.5 nm width), without significant intersolvent mixing. The aqueous interface with ILs is in fact an ill-defined heterogeneous domain, involving IL ions unconnected to the IL phase, surrounded by water, and water molecules on the IL side of the interface, unconnected to bulk water. There is thus no firm definition of complexes “at the interface” or “extracted” to the IL.

With these features in mind, it is noteworthy to observe during the dynamics extraction of strontium complexes to the IL phase. Such events did not occur at the chloroform interface.⁶⁵ Furthermore, extraction is found to depend on the state of nitrate

counterions and on the IL. In the case of the $[C_4mim][PF_6]$ IL, one observes the extraction of either charged $[Sr\subset 18C6]^{2+}$ or neutral $[Sr\subset 18C6(NO_3)_2]$ species, expected respectively in the case of ion exchange and classical extraction mechanisms. The different amounts of C_4mim^+ cations and PF_6^- anions in the bulk water phases (see Table 5) also nicely reflect the two types of extraction mechanisms: with the two tested water models, there are more C_4mim^+ cations in bulk water with the charged than with the neutral complexes. Furthermore, in bulk water, with both water models, C_4mim^+ cations are more concentrated than PF_6^- anions in the case of charged $[Sr\subset 18C6]^{2+}$ complexes, but have similar concentrations in the case of the neutral complexes. Although we cannot conclude on which mechanism is preferred, these features clearly follow expected trends with the two mechanisms.

In the case of the $[C_8mim][PF_6]$ /water biphasic system, no C_8mim^+ cation is solubilized in water, which precludes a cation exchange mechanism. In fact, during the simulation of system E, a remarkable extraction process occurred: migration of the charged complex toward the interface, neutralization upon complexation of nitrate, and diffusion of the complex to the IL phase. No charged complex was extracted during that simulation. The results fully support the classical extraction mechanism to the $[C_8mim][PF_6]$ IL. Regarding the lack of spontaneous Sr extraction via neutral complexes to $[C_8mim][PF_6]$, this may be due to several features: (i) still insufficient sampling, (ii) possible barrier for interface crossing, or (iii) oversimplification of the system (e.g., neglect of salting-out or acidity effects).⁶⁴

To conclude, simulations of Sr complexes at aqueous interfaces with ionic liquids reveal very different landscapes, compared to those at the corresponding classical interfaces. In spite of computational limitations (relatively small solvent boxes, sampling issues, and simple force field representation of the systems; see e.g. discussions in refs 66–69), the calculated distributions of the complexes and IL ions support different extraction mechanisms depending on the IL. To the best of our knowledge, this is the first computational MD report on the spontaneous transfer of complexed ions a LLE system. Further insights can be obtained by calculation of free energy profiles for interface crossing of the different species to the different ILs (PMF calculations).^{56,70} As stressed from the present study, adequate sampling at every step will be a major challenge.

Acknowledgment. The authors are grateful to IDRIS, CINES, Université de Strasbourg, and GDR CNRS PARIS for computer resources and to E. Engler for assistance. They also acknowledge G. Chevrot for exploratory simulations on these systems.

Supporting Information Available: Figures with atomic charges, initial biphasic system, solvent RDF's, and snapshots of demixing simulations. This material is available free of charge via the Internet at <http://pubs.acs.org>.

References and Notes

- Wilkes, J. S.; Zaworotko, M. J. *J. Chem. Soc., Chem. Commun.* **1992**, 965–967.
- Welton, T. *Chem. Rev.* **1999**, 99, 2071–2083.
- Wassercheid, P.; Keim, W. *Angew. Chem. Int. Ed.* **2000**, 39, 3772–3789.
- Visser, A. E.; Swatloski, R. P.; Reichert, W. M.; Griffin, S. T.; Rogers, R. D. *Ind. Eng. Chem. Res.* **2000**, 39, 3596–3604.
- Visser, A. E.; Swatloski, R. P.; Griffin, S. T.; Hartman, D. H.; Rogers, R. D. *Sep. Sci. Technol.* **2001**, 36, 785–804.
- Wei, G. T.; Yang, Z.; Chen, C. *J. Anal. Chim. Acta* **2003**, 488, 183–192.
- Dietz, M. L.; Dzielawa, J. A.; Jensen, M. P.; Beitz, J. V.; Borkowski, M. In *Ionic liquids IIIB: fundamentals, progress, challenges and opportunities. Transformations and processes*; Rogers, R. D., Seddon, K. R., Eds.; American Chemical Society: Washington, DC, 2005; Chapter 1, pp 2–18 and references cited therein.
- Chun, S.; Dzyuba, S. V.; Bartsch, R. A. *Anal. Chem.* **2001**, 73, 3737–3741.
- Luo, H.; Bonnesen, P. V. *Anal. Chem.* **2004**, 76, 2773–2779.
- Luo, H.; Dai, S.; Bonnesen, P. V.; Buchanan III, A. C.; Holbrey, J. D.; Bridges, N. J.; Rogers, R. D. *Anal. Chem.* **2004**, 76, 3078–3083.
- Visser, A. E.; Rogers, R. D. *J. Solid State Chem.* **2003**, 171, 109–113.
- Gutowski, K. E.; Bridges, N. J.; Cocalia, V. A.; Spear, S. K.; Visser, A. E.; Holbrey, J. D.; Davis, J. H.; Rogers, R. D. In *Ionic liquids IIIA: fundamentals, progress, challenges and opportunities. Properties and structure*; Rogers, R. D., Seddon, K. R., Eds.; American Chemical Society: Washington, DC, 2005; Chapter 3, p 33.
- Harjani, J. R.; Friscic, T.; MacGillivray, L. R.; Singer, R. D. *Dalton Trans.* **2008**, 4595–4601.
- Ouadi, A.; Klimchuk, O.; Gaillard, C.; Billard, I. *Green Chem.* **2007**, 9, 1160–1162.
- Visser, A. E.; Swatloski, R. P.; Reichert, W. M.; Mayton, R.; Sheff, S.; Wierzbicki, A.; Davies, J.; Rogers, R. D. *Chem. Commun.* **2001**, 2523–2529.
- Dai, S.; Ju, Y. H.; Barnes, C. E. *J. Chem. Soc., Dalton Trans.* **1999**, 1201–1202.
- Dietz, M. L.; Dzielawa, J. A. *Chem. Commun.* **2001**, 2124–2125.
- Dietz, M. L.; Dzielawa, J. A.; Laszak, I.; Young, B. A.; Jensen, M. P. *Green Chem.* **2003**, 5, 682–685.
- Luo, H.; Dai, S.; Bonnesen, P. V.; Haverlock, T. J.; Moyer, B. A.; Buchanan III, A. C. *Solvent Extr. Ion Exch.* **2006**, 24, 19–31.
- Yuan, L. Y.; Peng, J.; Xu, L.; Zhai, M. L.; Li, J. Q.; Wei, G. S. *J. Phys. Chem. B* **2009**, 113, 8948–8952.
- Jensen, M. P.; Neufeld, J.; Beitz, J. V.; Skanthakumar, S.; Soderholm, L. *J. Am. Chem. Soc.* **2003**, 125, 15466–15473.
- Dietz, M. L.; Jakab, S.; Yamato, K.; Bartsch, R. A. *Green Chem.* **2008**, 10, 174–176.
- We previously reported a 4 ns MD study on Sr complexes with 18C6 at the $[C_4mim][PF_6]$ /water interface (Vayssiére, P.; Chaumont, A.; Wipff, G. *Phys. Chem. Chem. Phys.* **2004**, 7, 124). The present study differs by several features. Regarding the studied systems: here, we focus on the extraction mechanism and compare two ILs and two forms of the complexes involved in the different mechanisms. Regarding the methodology: (i) For the electrostatic representation of the system, we use atomic charges fitted on every complex to account for the charge redistribution upon complexation, including polarization of the ligands and charge transfer effects. The Sr^{II} charge and the NO_3^- charges are thus reduced and the complexes are less polar, possibly facilitating their extraction. (ii) The sampling has been significantly improved by calculating long MD trajectories at preformed interfaces (up to 100 ns per system), and by simulating random mixtures of solvents and solutes (mixing–demixing simulations).
- Anthony, J. L.; Maginn, E. J.; Brennecke, J. F. *J. Phys. Chem. B* **2001**, 105, 10942–10949.
- Jensen, M. P.; Beitz, J. V.; Neufeld, J.; Skanthakumar, S.; Soderholm, L. In *Ionic liquids IIIA: fundamentals, progress, challenges and opportunities. Properties and structure*; Rogers, R. D., Seddon, K. R., Eds.; American Chemical Society: Washington, DC, 2005; Chapter 2, pp 18–19.
- Case, D. A.; Pearlman, D. A.; Caldwell, J. W.; Cheatham III, T. E.; Wang, J.; Ross, W. S.; Simmerling, C. L.; Darden, T. A.; Merz, K. M.; Stanton, R. V.; Cheng, A. L.; Vincent, J. J.; Crowley, M.; Tsui, V.; Gohlke, H.; Radmer, R. J.; Duan, Y.; Pitera, J.; Massova, I.; Seibel, G. L.; Singh, U. C.; Weiner, P. K.; Kollman, P. A. *AMBER 7.0*; University of California: San Francisco, 2002.
- de Andrade, J.; Böes, E. S.; Stassen, H. *J. Phys. Chem. B* **2002**, 106, 13344–13351.
- Kaminski, G. A.; Jorgensen, W. L. *J. Chem. Soc., Perkin Trans. 2* **1999**, 2, 2365–2375.
- de Andrade, J.; Böes, E. S.; Stassen, H. *J. Phys. Chem. B* **2002**, 106, 3546–3548.
- Chaumont, A.; Engler, E.; Wipff, G. *Inorg. Chem.* **2003**, 42, 5348–5356.
- Liu, Z.; Huang, S.; Wang, W. *J. Phys. Chem. B* **2004**, 108, 12978–12989.
- Chaumont, A.; Schurhammer, R.; Wipff, G. *J. Phys. Chem. B* **2005**, 109, 18964–18973.
- Jorgensen, W. L.; Chandrasekhar, J.; Madura, J. D.; Impey, R. W.; Klein, M. L. *J. Chem. Phys.* **1983**, 79, 926–936.
- Berendsen, H. J. C.; Grigera, J. R.; Straatsma, T. P. *J. Phys. Chem.* **1987**, 91, 6269–6271.
- Åqvist, J. *J. Phys. Chem.* **1990**, 94, 8021–8024.
- Baaden, M.; Burgard, M.; Wipff, G. *J. Phys. Chem. B* **2001**, 105, 11131–11141.

- (37) Cornell, W. D.; Cieplak, P.; Bayly, C. I.; Gould, I. R.; Merz, K. M.; Ferguson, D. M.; Spellmeyer, D. C.; Fox, T.; Caldwell, J. W.; Kollman, P. A. *J. Am. Chem. Soc.* **1995**, *117*, 5179–5197.
- (38) Darden, T. A.; York, D. M.; Pedersen, L. G. *J. Chem. Phys.* **1993**, *98*, 10089.
- (39) Berendsen, H. J. C.; Postma, J. P. M.; van Gunsteren, W. F.; DiNola, A. *J. Chem. Phys.* **1984**, *81*, 3684–3690.
- (40) Gu, Z.; Brennecke, J. F. *J. Chem. Eng. Data* **2002**, *47*, 339.
- (41) Rickert, P. G.; Stepiniski, D. C.; Rausch, D. J.; Bergeron, R. M.; Jakab, S.; Dietz, M. L. *Talanta* **2007**, *72*, 315–320.
- (42) Engler, E.; Wipff, G. In ; Tsoucaris, G., Ed.; Kluwer: Dordrecht, The Netherlands, 1996; pp 471–476.
- (43) Benjamin, I. *Annu. Rev. Phys. Chem.* **1997**, *48*, 407–451.
- (44) Vayssi  re, P.; Chaumont, A.; Wipff, G. *Phys. Chem. Chem. Phys.* **2004**, *7*, 124–135.
- (45) Chaumont, A.; Wipff, G. *Inorg. Chem.* **2004**, *43*, 5891–5901.
- (46) Sieffert, N.; Wipff, G. *J. Phys. Chem. A* **2006**, *110*, 1106–1117.
- (47) The calculated ΔE_{tot} energy preference for $[\text{Sr} \subset 18\text{C}6(\text{NO}_3)_2]$, compared to the $[\text{Sr} \subset 18\text{C}6]^{2+}$ containing solutions, is larger in dry $[\text{C}_4\text{mim}][\text{PF}_6]$ than in dry $[\text{C}_8\text{mim}][\text{PF}_6]$ IL (by –150 and –50 kcal/mol, respectively), and smallest in the humid $[\text{C}_4\text{mim}][\text{PF}_6]$ IL (16 kcal/mol).
- (48) Jensen, M. P.; Dzielawa, J. A.; Rickert, P.; Dietz, M. L. *J. Am. Chem. Soc.* **2002**, *124*, 10664–10665.
- (49) Lynden-Bell, R. M.; Kohanoff, J.; Popolo, M. G. D. *Faraday Discuss.* **2005**, *129/5*, 1–11.
- (50) Chevrot, G.; Schurhammer, R.; Wipff, G. *Phys. Chem. Chem. Phys.* **2006**, *8*, 4164–4174.
- (51) Benjamin, I. *Science* **1993**, *261*, 1558–1560.
- (52) As mentioned in the Methods section, the charge reduction mimicking the charge transfer to Sr^{II} within the complex diminishes the Coulombic attractions between Sr^{II} , the crown and the nitrates. This is why the neutral complexes have been modeled with $\text{Sr}-\text{O}$ pseudobonds.
- (53) Watarai, H. *Trends Anal. Chem.* **1993**, *12*, 313–318.
- (54) Among the 10 complexes found within 7.5 Å from the interface (4 at ITF_A and 6 at ITF_B), the majority (90 %) sit on the water side and cannot thus be extracted. Furthermore, during the dynamics, two $[\text{Sr}-18\text{C}6]^{2+}$ species decomplexed and the freed 18C6 diffused to the interface.
- (55) Troxler, L.; Wipff, G. *Anal. Sci.* **1998**, *14*, 43–56.
- (56) Lauterbach, M.; Engler, E.; Muzet, N.; Troxler, L.; Wipff, G. *J. Phys. Chem. B* **1998**, *102*, 225–256.
- (57) Wipff, G.; Lauterbach, M. *Supramol. Chem.* **1995**, *6*, 187–207.
- (58) Schurhammer, R.; Berny, F.; Wipff, G. *Phys. Chem. Chem. Phys.* **2001**, *3*, 647–656.
- (59) Interactions energies with chloroform and water are respectively –573 and –2033 kcal/mol for the $[\text{Sr} \subset 18\text{C}6(\text{NO}_3)_2]$ complexes and, respectively, –636 and –1820 kcal/mol for the $[\text{Sr} \subset \text{DCH}18\text{C}6(\text{NO}_3)_2]$ complexes. As expected, the $[\text{Sr} \subset \text{DCH}18\text{C}6(\text{NO}_3)_2]$ complexes are thus somewhat less attracted by water and have a higher proportion on the chloroform side of the interface (52%) than the $[\text{Sr}-18\text{C}6(\text{NO}_3)_2]$ complexes (10%). They should thus be more easily transferred to chloroform.
- (60) Vandegrift, G. F.; Lewey, S. M.; Dytkacz, G. R.; Horwitz, E. P. *J. Inorg. Nucl. Chem.* **1980**, *42*, 1359–1361.
- (61) Szymankowski, J. *Solvent Extr. Ion Exch.* **2000**, *18*, 729–751.
- (62) Prochaska, K. *Adv. Colloid Interface Sc.* **2002**, *95*, 51–72.
- (63) Sieffert, N.; Chaumont, A.; Wipff, G. *J. Phys. Chem. C* **2009**, *113*, 10610–10622.
- (64) Experimentally, classical extraction of Sr^{2+} by DCH18C6 has been reported to proceed from an acidic aqueous phase (salting-out effect of NO_3^- ions). Without acid, there is almost no extraction. The lack of extraction to chloroform in our simulations may thus also be due to the lack of acid or salting-out agent in the aqueous phase. This result markedly contrasts with the spontaneous transfer of some complexes to the IL in the simulations without acid. To further test the effect of added acid in the classical system, we simulated system N (defined in Table 1) with 5 M nitric acid in the aqueous phase, $[\text{Sr} \subset \text{DCH}18\text{C}6(\text{NO}_3)_2]$ complexes and free DCH18C6 ligands in chloroform. In fact, at the end of the dynamics, one can see an equilibrium between complexes adsorbed at the interface and extracted complexes, solvated by HNO_3 species (Figure 8).
- (65) Arguably, simulation times at the chloroform/water interface (10 ns) are shorter than those of the IL/water interfaces (up to 100 ns). In the former case, however, the system is equilibrated, as seen from the comparison of mixing–demixing simulation results (within ca. 1 ns) with those obtained at preformed interfaces (Muzet, N.; Wipff, G., *J. Phys. Chem. B* **1998**, *102*, 10772–10788). As seen in this paper, in the case of ILs, both types of approaches do not converge to identical landscapes.
- (66) Sieffert, N.; Wipff, G. *J. Phys. Chem. B* **2006**, *110*, 13076–13085.
- (67) Del Popolo, M. G.; Kohanoff, J.; Lynden-Bell, R. M.; Pinilla, C. *Acc. Chem. Res.* **2007**, *40*, 1156–1164.
- (68) Yan, T.; Burnham, C. J.; Popolo, M. G. D.; Voth, G. A. *J. Phys. Chem. B* **2004**, *108*, 11877–11881.
- (69) Chang, T.-M.; Dang, L. X. *J. Phys. Chem. A* **2009**, *113*, 2127–2135.
- (70) Wick, C. D.; Dang, L. X. *Chem. Phys. Lett.* **2008**, *458*, 1–5.

JP106441H